

Exhibit A

“Jørgensen”

Applicant: Grønborg *et al.*

Serial No.: 10/594,192

Characterization of Meteorin—An Evolutionary Conserved Neurotrophic Factor

Jesper Roland Jørgensen · Lachlan Thompson ·
Lone Fjord-Larsen · Christina Krabbe · Malene Torp ·
Nisse Kalkkinen · Claus Hansen · Lars Wahlberg

Received: 22 December 2008 / Accepted: 16 February 2009
© Humana Press 2009

Abstract Growth factors control cellular growth, proliferation, and differentiation and may have therapeutic applications. In this study, we focus on Meteorin which is a member of a largely uncharacterized evolutionary conserved two-member growth factor family. Our analysis shows that Meteorin is expressed in the central nervous system both during development and in adult mice. Detailed immunohistological analysis of the adult mouse brain reveals that Meteorin is highly expressed in Bergmann glia and in a few discrete neuronal populations residing in the superior colliculus, the ocular motor nucleus, the raphe and pontine nuclei, and in various thalamic nuclei. In addition, low levels of Meteorin is found in

astrocytes (S100 β +, OX42-) distributed ubiquitously throughout the brain. Meteorin was cloned and recombinant protein purified allowing N-terminal sequencing and mass spectrometric analysis showing that Meteorin is secreted as an unmodified monomer. This form is bioactive as it induces neurite outgrowth from dorsal root ganglions in vitro. Intrastriatal protein injection and lentiviral studies in vivo showed that Meteorin is a highly diffusible molecule in the brain and cellular uptake is apparent in specific populations which may carry the receptor. In summary, we provide a comprehensive expression analysis and have made and thoroughly validated molecular tools to help investigate the therapeutic potential of Meteorin.

J. R. Jørgensen (✉) · L. Fjord-Larsen · C. Krabbe · M. Torp ·
L. Wahlberg
NaGene A/S,
Baltorvej 154,
2750 Ballerup, Denmark
e-mail: JRJ@nsgene.dk

L. Thompson
Wallenberg Neuroscience Center,
Department of Experimental Medical Research, Lund University,
221 84 Lund, Sweden

C. Krabbe
Anatomy & Neurobiology, University of Southern Denmark,
Winslowparken 21,
5000 Odense, Denmark

N. Kalkkinen
Institute of Biotechnology, Protein Chemistry Research Group,
University of Helsinki,
00014 Helsinki, Finland

C. Hansen
The Wilhelm Johansson Centre for Functional Genome Research,
IMBG, Panum Institute, University of Copenhagen,
2200 Copenhagen, Denmark

Keywords Growth factor · Biologies · Expression ·
Gene therapy · In vivo delivery

Abbreviations

5HT	5-Hydroxytryptamine
CDNF	Conserved dopamine neurotrophic factor
ChAT	Choline acetyltransferase
ESI-MS	Electrospray ionization mass spectrometry
GDNF	Glial-derived neurotrophic factor
GFAP	Glial fibrillary acidic protein
IHC	Immunohistochemistry
ISH	In situ hybridization
LC-ESI-MS/MS	Liquid chromatography electrospray ionization tandem mass spectrometry
MALDI-TOF	Matrix-assisted laser desorption/ionization time-of-flight
METRN	Meteorin, glial cell differentiation regulator
NGF	Nerve growth factor
RP	Reverse phase
SC	Superior colliculus

Introduction

Neurotrophic growth factors are responsible for the growth and survival of neurons during development and for the maintenance of adult neurons. Furthermore, many of these factors may also be capable of repairing damaged neuronal populations in the adult and have therapeutic potential for disorders of the central nervous system, including Alzheimer's disease (Schindowski et al. 2008), Parkinson's disease (Evans and Barker 2008), and amyotrophic lateral sclerosis (Ekesten 2004). Even though many important factors have been discovered and are under development as therapeutics, the discovery of novel neurotrophic growth factors such as conserved dopamine neurotrophic factor (Lindholm et al. 2007) illustrates the continued importance of the discovery and detailed characterization of these types of molecules.

With the aim of finding novel or uncharacterized neurotrophic factors with therapeutic potential, we applied bioinformatic tools to the human, mouse, and rat genomes. One molecule identified using this approach is Meteorin, glial cell differentiation regulator (METRN), which has been described by Nishino and co-workers as a secreted protein upregulated in an embryonic carcinoma cell line upon exposure to retinoic acid (Nishino et al. 2004). The expression in the adult brain is not well described but, during development, the METRN transcript appears both in the central and peripheral nervous system with the most prominent levels in neural progenitors, glial progenitors, and cells of the astrocyte lineage. METRN is a potent neurotrophic growth factor that induces axonal outgrowth of sensory neurons and, like many other proteins in this category, it also affects glial cell differentiation (Nishino et al. 2004). Since its discovery, only one additional paper has been published on METRN reporting cerebral antiangiogenic activity and promotion of vascular maturation (Park et al. 2008).

To be able to ultimately address the therapeutic potential of METRN, initial basic research is needed. Therefore, we set out to comprehensively characterize expression and to make and validate reagents necessary for molecular and functional characterization. Initially, messenger RNA (mRNA) expression levels were analyzed by semi-quantitative reverse transcriptase polymerase chain reaction (RT-PCR) and Western blotting followed up by a detailed immunohistochemical analysis of the adult mouse brain. METRN was then cloned and recombinant protein produced and purified for biochemical characterization of the molecule as well as functional testing in dorsal root ganglion explant cultures. Furthermore, rat striatal injections of recombinant METRN and lentivirus expressing METRN were made to evaluate important *in vivo* delivery issues such as diffusion, uptake, and transport.

Methods

RNA, Complementary DNA, and Reverse Transcriptase Polymerase Chain Reaction RNA from mouse tissues was prepared by Zymogen (San Diego, CA, USA). All RNA samples were treated with RNase-free DNase to remove residual DNA and precisely quantified by triplicate spectrophotometry. RNA integrity was verified by denatured agarose gel electrophoresis and RNA purity assessed by A260/A280 measurements demonstrating ratios greater than 1.8 for all samples. For each tissue, exactly 2.5 µg RNA was used as template for complementary DNA (cDNA) synthesis with an RNaseH deficient reverse transcriptase derived from MoMLV (SuperScript) and a poly-dT primer. Two individual batches of cDNA were made and semi-quantitative RT-PCR done twice on each batch of cDNA as described previously (Jorgensen et al. 2006) with relevant plasmid DNA as standard to ensure detection within the dynamic range of the PCR reaction. METRN transcript was detected using the primers METRN_s (5'-GGTAGCCACGCTCTTCTTCG-3') and METRN_{as} (5'-CTGGGTACAGCCACTCGATAG-3') resulting in a 173-bp fragment. To confirm equal amount of template in the PCR reactions, GAPDH was detected using GAPDH_s (5'-AACAGCACTCCCACTCTTC-3') and GAPDH_{as} (5'-TGGTCCAGGGTTCCTACTC-3'). PCR product identity was verified by agarose gel electrophoresis and DNA sequencing (MWG Biotech AG, Germany). Furthermore, primers were designed to discriminate between the three splice variants of METRN originally submitted to NCBI as Hyrac (long: DQ133462, mid: DQ133463, and short: DQ133464). The long transcript encodes METRN (NP_598480) as described in this paper and as identified by Nishino et al. (2004). The primer set (mMETRNx_s: 5'-TCACGCTGGCTACTCGGAAGACC-3'/mMETRNx_{as}: 5'-TGCAGCTCTGTGTCATGGGCGACC-3') produce PCR products of 637, 345, and 264 bp for the three splice variants, respectively.

Primers were designed using Clone Manager 9 Professional Edition from Sci Ed Software (Cary, NC, USA) or Oligo (Molecular Biology Insights, Cascade, CO, USA) and ordered from TAG Copenhagen A/S, Denmark.

Sodium Dodecyl Sulfate Polyacrylamide Gel Electrophoresis and Western Blotting Protein samples were loaded on 12% or 15% homogenous sodium dodecyl sulfate polyacrylamide gel electrophoresis (SDS-PAGE) gels, electrophoresed, and stained with PhastGel™ Blue R (GE Healthcare, Uppsala, Sweden) according to the manufacturer's instructions or electroblotted to PVDF membranes for Western analysis. METRN was detected using a polyclonal goat antibody against recombinant mouse METRN (R&D Systems, AF3475) at 0.5 µg/ml as primary antibody and horseradish peroxidase (HRP)-linked anti-

goat (Dako; 1:2,000) as secondary antibody. Omission of primary antibody served as a negative control. Two mouse mixed tissue Western blots (Zyagen, MW-MT-1) and three mouse neuronal tissue Western blots (Zyagen, MW-200) were used for evaluation of METRN protein expression.

Cloning The coding sequence of METRN from mouse (NM_133719) was PCR cloned *Bam*HI/*Xho*I in pNS1n (Jensen et al. 2002) with a 5' Kozak sequence. C-terminal histidine tagging was done by including a sequence encoding GSGSGSHHHHH in the reverse primer. For production of lentivirus, the above *Bam*HI/*Xho*I fragments were transferred into pHSCXW as previously described (Leander et al. 2005). All constructs were verified by DNA sequencing (MWG Biotech AG, Germany).

Production of Recombinant Mouse METRN FreeStyle™ 293-F suspension cells (Invitrogen) were transfected with 1 mg pNS1n-mMETRN-HIS DNA per liter using Lipofectamine 2000 (Life Technologies). The culture was incubated with agitation at 37°C and 8% CO₂ for 4 days and separated into cell pellet and supernatant by centrifugation. The supernatant was sterile-filtered and recombinant protein purified with TALON Metal Affinity Resin (Clontech) followed by PD-10 gel filtration (GE Healthcare). The recombinant protein was stored at -80°C in pure phosphate-buffered saline (PBS) or in PBS + 0.1% HSA.

Reversed Phase High-Performance Liquid Chromatography Reversed phase chromatography was done on an Ultimate™ Micro HPLC system connected to a Probot™ Micro fraction collector (Dionex Corporation, USA) using a C4 column (1 × 150 mm, Phenomenex Jupiter, C4, 5 µm, 300 Å). The elution was performed with a linear gradient (0–100% in 60 min) of acetonitrile in 0.1% TFA using a flow rate of 50 µl/min and detection at 214 nm.

N-terminal Sequencing N-terminal sequence analysis of RP-purified recombinant mMETRN-HIS was done by Edman degradation using a Procise 494A HT Sequencer (Perkin Elmer, Applied Biosystems Division, CA, USA).

Mass Spectrometry Matrix-assisted laser desorption/ionization time-of-flight (MALDI-TOF) mass spectrometry was performed using an Ultraflex TOF/TOF instrument (Bruker Daltonik, Bremen, Germany) and electrospray ionization mass spectrometry (ESI-MS or LC-ESI-MS/MS) using a Q-TOF instrument (Micromass Ltd, Manchester, UK) connected to an Ultimate™ nano chromatograph (Dionex Corporation, USA). For total mass determination, protein fractions from RP chromatography were, either directly (Ylonen et al. 1999) or after reduction with DTT, alkylation with 4-vinylpyridine and desalting by RP (Nakari-Setälä et

al. 1996), subjected to MALDI-TOF analysis or ESI-MS analysis. For MALDI-TOF peptide mass fingerprinting, mMETRN-HIS bands from SDS-PAGE were "in gel" digested essentially as described by Shevchenko et al. (1996). Briefly, proteins (1–2 µg) were reduced with dithiothreitol and alkylated with iodoacetamide before digestion with trypsin (Sequencing Grade Modified Trypsin, V5111, Promega). The recovered peptides were then analyzed as described earlier (Poutanen et al. 2001).

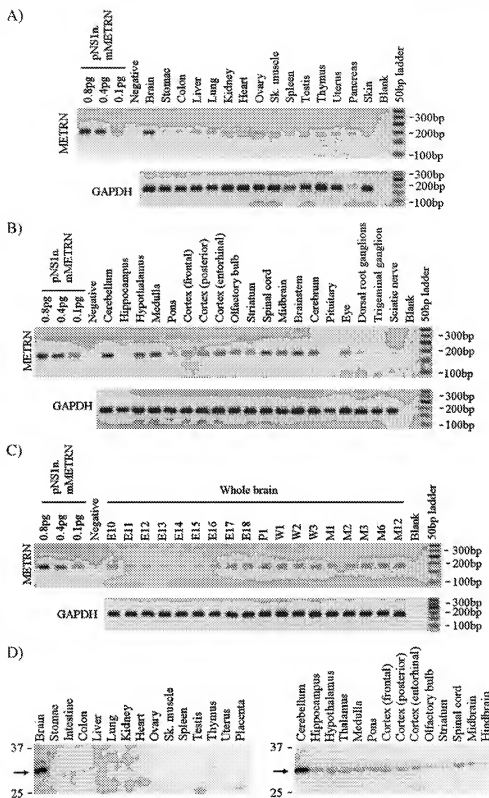
Striatal Injection of Recombinant Protein and Lentivirus All work involving animals was conducted in accordance with the Danish Animal Protection Law and with experimental procedures approved by the Danish National Committee for Ethics in Animal Research.

Young female Wistar Hannover Galas rats, HanTac:WH (Taconic, Denmark) weighing approximately 220 g, were used and housed under a 12-h light/dark cycle with free access to rat chow and water. Protein and lentiviral injections were performed under general anesthesia using isoflurane (1.5–2%). Animals were injected with either METRN protein (1.4 µg/animal) or rLV vector (2 × 10⁵ TU/animal) carrying the cDNA for WT or His-tagged mMETRN (*n*=6 per group). Using a Hamilton micro-syringe with a pulled glass pipette tip, four deposits (0.5 µl/deposit) of protein or lentivirus were injected into the striatum along two needle tracts at the following coordinates: track 1: AP=1.4 mm, ML=-2.6 mm with respect to bregma and DV₁=-5.0 and DV₂=-4.0 with respect to dura; track 2: AP=0.0 mm, ML=-3.7 mm, DV₁=-5.0 and DV₂=-4.0. The tooth bar was set at -2.3. Rats injected with protein were sacrificed after 2–3 h, whereas rats injected with lentivector were sacrificed after 2 weeks to allow transgenic METRN expression.

Immunohistochemistry The immunohistochemical analysis was performed using brain tissue from the rats described above as well as adult mouse brain tissue (female, NMRI wild-type) according to previously described procedures (Thompson et al. 2005). Briefly, deeply anesthetized animals received transcardial perfusions of 0.9% saline followed by 4% paraformaldehyde (PFA), brains were removed and post-fixed overnight in 4% PFA and then cryo-protected in 25% sucrose in 0.1 M phosphate buffer for 48 h. Mouse brains were cut on a freezing microtome at 30 µm in 12 series in either the coronal or sagittal plane. Rat brains were cut in six series of 40 µm coronal sections. Free-floating sections were incubated at room temperature overnight with primary antibody diluted in 0.1 M potassium phosphate buffered saline (KPBS) with 0.25% Triton X-100 and 5% normal donkey serum (NDS) or normal horse serum (NHS). Primary antibodies and dilutions used in this study were as follows: rabbit anti-5-hydroxytryptamine

Figure 1 Semi-quantitative RT-PCR (a–c) and Western blot analysis (d) of METRN expression in mouse tissues.

a Among 15 adult mouse tissues, METRN mRNA is found primarily in the brain. b METRN mRNA expression in 19 subdissected adult mouse CNS and PNS tissues. c METRN mRNA is found in whole brain preparations throughout development. *E* embryonic day, *P* postnatal day, *W* weeks postnatal, *M* months postnatal. d Anti-METRN Western analysis of 29 subdissected adult mouse tissues showing that METRN is expressed only in the CNS. Note agreement between RT-PCR data (a, b) and Western analysis (d)



(5HT; Incstar; 1:10,000), rabbit anti-calbindin (Swant; 1:1,000), mouse anti-choline acetyltransferase (ChAT; Chemicon; 1:1,000), rabbit anti-GABA (Sigma; 1:500), rabbit anti-GFAP (Dako; 1:1,000), goat anti-Metecorin

(R&D Systems; 1:500), mouse anti-NuN (Chemicon; 1:1,000), mouse anti-OX42 (Serotec; 1:100), mouse anti-parvalbumin (Sigma; 1:2,000), and mouse anti-S100 β (Sigma; 1:100). For fluorescent double labeling, the

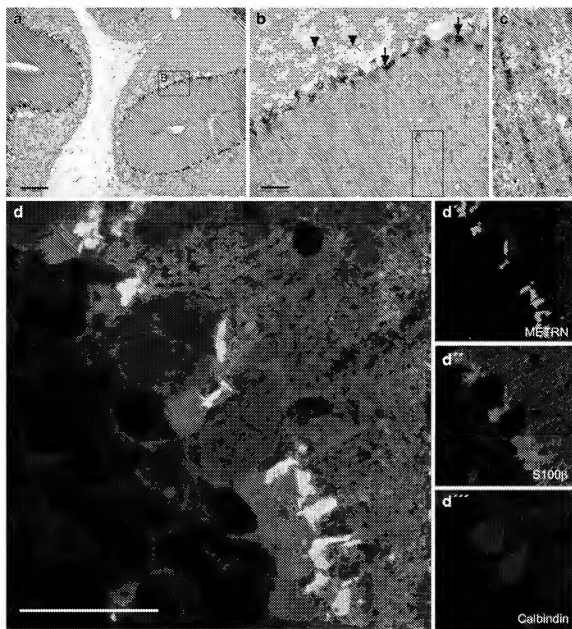
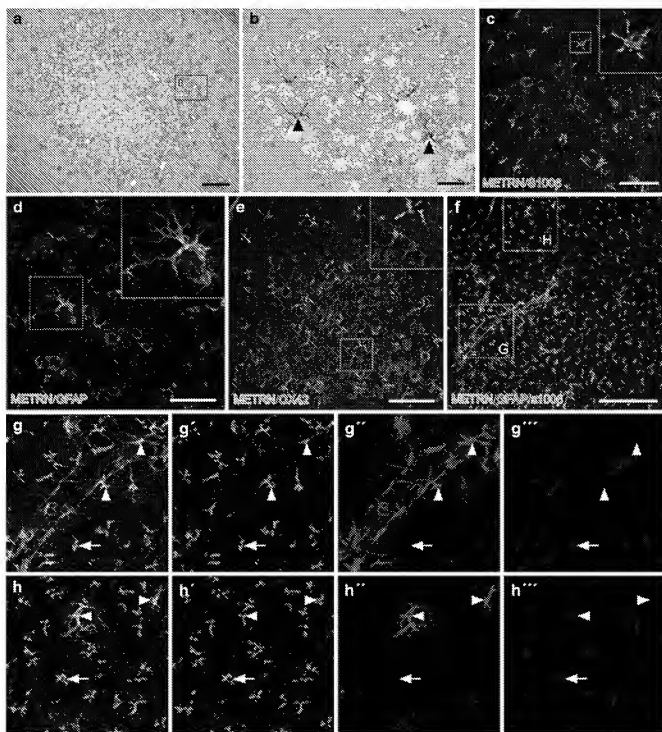


Figure 2 Immunohistochemical analysis of METRN expression in the adult mouse cerebellum. *A* Intensely labeled METRN expressing cells can be seen in the Purkinje cell layer of the cerebellum. *B* The boxed area in *A* shown at higher magnification illustrates high expression in the Purkinje layer in greater detail (arrows) and also shows that cells in the granular layer express a lower level of METRN (arrowheads). *C*

Radial processes extending into the molecular layer are decorated with METRN in a punctuate pattern (expanded from boxed area in *B*). *D* Triple labeling shows that METRN (green) is expressed by S100 β + (red) cells that are interspersed between calbindin+ (blue) Purkinje neurons. *D'*–*D'''* Image from *D* represented as single color channels. Scale bars represent 100 μ m (*A*), 20 μ m (*B*), or 25 μ m (*D*)

antibody–antigen complexes were visualized through incubation (2 h) in KPBS with 2% NDS, 0.25% triton X-100 and the appropriate combinations of the following secondary antibodies: Cy2 donkey anti-goat; Cy3 donkey anti-rabbit; Cy3 donkey anti-mouse; Cy5 donkey anti-rabbit; and Cy5 donkey anti-mouse (all 1:200; Jackson ImmunoResearch). Single labeling of METRN was achieved through incubation of the primary antibody-

labeled sections with biotinylated horse anti-goat in KPBS (+2% NHS, 0.25% triton X-100) for 2 h followed by conjugation of HRP using a streptavidin–HRP complex (ABC elite kit, Vector Laboratories), incubation with 3,3'-diaminobenzidine (DAB), and precipitation of the chromophore with 1% H₂O₂. For peroxidase-based immunochemical procedures, sections were quenched of endogenous peroxidase activity through incubation with 3% H₂O₂ prior to



◀ **Figure 3** Immunohistochemical analysis of METRN expression in the adult mouse cortex. *A* METRN⁺ cells can be found diffusely throughout the cortex. *B* Higher magnification (boxed area from *A*) shows individual METRN⁺ cells with METRN expressed most prominently in cellular processes in a stellate pattern, while being absent or weakly expressed in the cell soma (arrowhead). *C–E* The vast majority of METRN⁺ cells with this morphology express S100 β (red in *C*) and a subset of these also express GFAP (red in *D*). There was no overlap between OX42⁺ microglia (red in *E*) and METRN expression. Boxed areas in *C–E* are expanded as insets. *F* Triple labeling of METRN (green), GFAP (red), and S100 β (blue) shows diffuse distribution of METRN⁺/S100 β ⁺ glia not expressing GFAP (boxed area expanded as *H–H'''*) as well as the clustering of GFAP expressing METRN⁺/S100 β ⁺ around a blood vessel (boxed area expanded as *G–G'''*). *G–G'''* Typical clustering of GFAP expressing astrocytes around a blood vessel—arrowheads denote GFAP⁺/METRN⁺ cells, arrows denote GFAP⁺/METRN[−] cells. Note that while some of the GFAP⁺ cells do not appear S100 β ⁺, this likely reflects that the cell soma is not included in the optical section and signal is from associated processes only. Our analysis has shown virtually all METRN⁺ cells to also express S100 β , irrespective of GFAP expression. *H–H'''* Most METRN⁺ cells in the cortical parenchyma express S100 β , but not GFAP (e.g., arrow), while occasional GFAP expressing cells can also be found (arrowheads). Scale bars represent 100 μ m (*A*), 20 μ m (*B*), 50 μ m (*C–E*), and 200 μ m (*F*)

application of the primary antibodies. Labeled sections were slide-mounted and cover-slipped for microscopic analysis.

Image Acquisition Fluorescent photographs were acquired using Leica DMRE laser-scanning confocal microscope equipped with green helium/neon, helium/neon, and argon lasers.

Dissociated Dorsal Root Ganglia Cultures Rat P5 dorsal root ganglions were dissociated using Papain Dissociation System (Worthington Biochemical Corp, USA) and were subsequently plated in polyornithine-coated 24-well plates in DMEM/F12 medium (Invitrogen) with 5% heat-inactivated horse serum (Seromed) at a cell density of 1.5×10^4 cells/cm². After 1 h, when the cells had attached, the medium was changed to serum-free DMEM/F12 with 1% gentamycin (Invitrogen) and the indicated additions of recombinant METRN or nerve growth factor (NGF; R&D Systems). Cells were incubated at 37°C and 5% CO₂ for 1 day and fixed in 4% PFA. Immunocytochemistry was performed on the fixed cultures using β -III-tubulin antibody (Sigma) diluted 1:15,000 in 1% normal horse serum and 0.1% Triton X-100 in PBS followed by biotinylated secondary antibody (horse-anti-mouse) followed by ABC Elite kit (Vector Laboratories), where after the color reaction was developed using DAB as chromogen. Neurite length per cell was quantified using Visio-Morph image analysis on at least nine images from triplicate wells. The experiment was repeated three times, and data shown are the means \pm SEM from a representative experiment.

Results

METRN Is Expressed in the Central Nervous System During Development and in Adults

To initially address expression, METRN mRNA levels were analyzed by semi-quantitative RT-PCR in a number of adult mouse tissues. In the adult animal, METRN is predominantly expressed in the brain but also detected in smaller amounts in other organs such as kidney, heart, ovary, and skeletal muscle (Fig. 1a). Within the adult mouse brain, METRN mRNA is widely expressed with the highest levels in cerebellum, medulla, and brainstem (Fig. 1b). High expression is also found in the spinal cord but METRN transcript levels are low in the adult peripheral nervous system. Steady or slightly increasing levels of METRN mRNA can be detected in the mouse brain during development (E10–E18), in pups (P1–W3), and in adult animals (M1–M12; Fig. 1c). Three splice variants of mMETRN have been reported to NCBI (long: DQ133462, mid: DQ133463, and short: DQ133464) where the longest encodes full length METRN as described by Nishino et al. (2004). The long splice variant is by far the most dominant form in the tissues examined in this study (data not shown).

To address the expression of METRN protein in adult mouse tissue, protein extracts were analyzed by Western blotting (Fig. 1d). METRN protein is detected only in the brain and not in other organs. Within the brain, the most prominent expression is found in the cerebellum but METRN is also detectable in virtually all other central nervous system (CNS) tissues in agreement with RT-PCR data.

METRN Is Highly Expressed in Bergmann Glia but Can also Be Found in Astrocytes Scattered Throughout the Mouse Brain

To investigate METRN protein expression at the cellular level, immunohistochemistry (IHC) analysis of the adult mouse brain was performed. Since METRN protein levels are highest in the cerebellum (Fig. 1d), this region was used for optimization and analyzed first. Intense staining of cell bodies in the Purkinje cell layer was observed with radial fibers projecting through the molecular layer to the pial surface (Fig. 2 A–C). To identify the cell type expressing METRN, triple labeling was done with S100 β to mark glia cells and calbindin to mark Purkinje neurons (Slemmon et al. 1985; Fig. 2 D). It is clear from this analysis that METRN is expressed by glial cells interspersed between Purkinje neurons. This is in line with the Bergmann glia which are radial glia similar to Müller cells of the retina where METRN mRNA has been previously detected (Nishino et al. 2004). Regarding the cellular distribution of METRN in these glial cells, it appears to be largely

excluded from the cell soma and found mainly in the cytoplasm along radial processes, as would be expected from a secreted protein. In addition to the intensely stained METRN expressing glia in the granule layer, we also observed more weakly stained METRN expressing cells, with glial morphology, throughout the cerebellar parenchyma (Fig. 2 B, arrowhead). Further analysis in other structures revealed that these cells were distributed fairly ubiquitously throughout the brain and upper brainstem, in agreement with RT-PCR and Western blot analysis of subdivided brain tissues (Fig. 1 B, D—right). Examples from frontal cortex are illustrated in Fig. 3. METRN expressing cells were diffusely distributed throughout the cortex (Fig. 3 A) displaying a glial morphology with METRN expression most prominent in the processes (Fig. 3 B). Further immunohistochemical analysis directed at proteins indicative of glial phenotype showed that virtually all METRN expressing glia also expressed S100 β (Fig. 3 C), and some expressed GFAP (Fig. 3 D), but there was no overlap with OX42 (Fig. 3 E), indicating an astrocytic rather than a microglial phenotype. The GFAP expressing METRN+ glia were often seen clustered around blood vessels throughout the brain (Fig. 3 F–H), consistent with the normal distribution of GFAP+ cells in the brain. However, despite the prominent appearance of this vasculature associated METRN+ signal, this was clearly a subset of a broader population of METRN expressing glia distributed throughout the brain.

METRN Is also Expressed in Defined Neuronal Subsets

In addition to the glial expression, we observed a number of prominent neuronal populations in discrete brain regions, with an intense METRN expression (Fig. 4). In particular, we observed METRN+ neuronal populations in the superficial layers of the superior colliculus (SC; Fig. 4 A–C), the ocular motor nucleus (Fig. 4 D–F), the raphe and pontine nuclei (Fig. 4 G, H), and also in various thalamic nuclei (Fig. 4 I). This pattern encompassed a variety of neuronal phenotypes. The size and morphology of the neurons in the SC was indicative of an interneuron identity and a number of these were found to also express GABA (Fig. 4 C). Consistent with an ocular motor neuron phenotype, METRN+ neurons in the ocular motor nucleus were large, rounded cells that also expressed ChAT (Fig. 4 F). The vast majority, if not all, METRN+ neurons throughout the raphe nucleus co-expressed 5HT (Fig. 4 H). METRN expression was quite widespread in neurons throughout the thalamus, although distinct groups of METRN+ neurons could be delineated based on the intensity of METRN expression (Fig. 4 I). These clusters of cells clearly corresponded to distinct thalamic nuclei as illustrated by counter-labeling with parvalbumin and calbindin. The highest expressing populations were found in the latero-posterior and reticular thalamic nuclei.

Production and Characterization of Recombinant METRN

To be able to study biochemical properties of METRN, recombinant mMETRN-HIS protein was produced in FreeStyle™ 293-F cells and purified by metal affinity chromatography. From reversed phase chromatography and SDS-PAGE analysis (Fig. 5a), it is evident that recombinant METRN is highly pure. The main peak from reversed phase chromatography was collected and used for N-terminal sequencing and mass spectrometric analysis.

N-terminal sequence analysis gave a pure sequence (GYSEDRCSWR...) in agreement with SignalP prediction (Bendtsen et al. 2004). The calculated molecular mass of the mMETRN-HIS polypeptide chain with the determined N-terminus and the additional C-terminal extension (...GSGSGSHHHHH) is 30,696.7 Da. If the protein contains five disulfide bridges, as expected from the primary sequence, the calculated mass is 30,686.7 Da. MALDI-TOF mass spectrometric analysis of METRN-HIS gave a mass value of 30,702 Da (Fig. 5b) which, within the mass accuracy of the analysis method, suggests that the polypeptide chain is a monomer and complete without any other posttranslational modifications than the possible disulfide bridges. This was further confirmed by ESI-Q-TOF mass spectrometric analysis (not shown) of the reduced, alkylated (4-vinylpyridine) METRN-HIS which gave a single pure mass of 31,749.0 Da (calculated mass including 10 pyridylethyl groups is 31,748.1 Da). METRN-HIS was further subjected to MALDI-TOF peptide mass fingerprinting and LC-ESI-MS/MS analyses which confirmed the major part (peptide coverage >60%) of the sequence, including the N- and C-termini. Furthermore, down to a few picograms, recombinant mMETRN-HIS is recognized by anti-Meteorin in the presence of 10% fetal calf serum (FCS; Fig. 5c).

METRN is known to promote neurite outgrowth from dorsal root ganglion explants (Nishino et al. 2004). To confirm biological activity of the recombinant mMETRN-HIS, it was tested in dissociated P5 rat dorsal root ganglion cultures (Fig. 5d). In this setup, mMETRN-HIS was bioactive and promoted neurite outgrowth to the same extent as NGF.

In Vivo Delivery of METRN

To be able to eventually evaluate the clinical potential of METRN in animal neurodegenerative disease models, in vivo delivery, diffusion, uptake, and transport are important issues. In order to study these mechanisms, we delivered recombinant mMETRN-HIS to the adult rat striatum through either direct injection of the recombinant protein (Fig. 6b–d) or via a lentiviral vector (Fig. 6e–j). Immunohistochemical analysis of tissue from rats, sacrificed 2 h

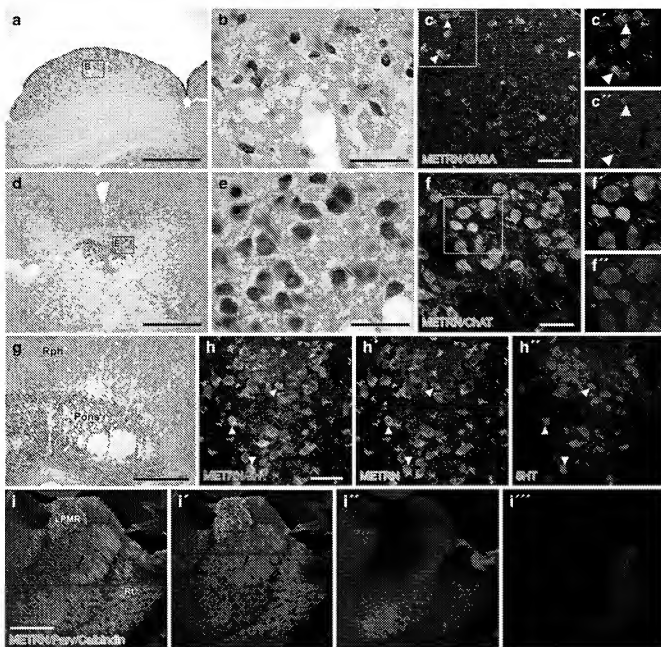
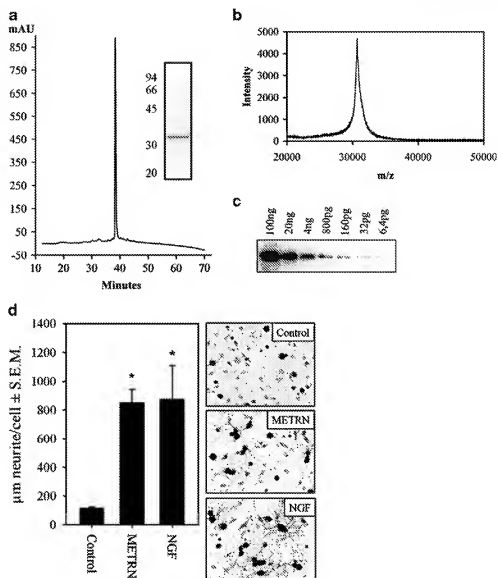


Figure 4 Immunohistochemical analysis reveals that METRN is expressed by discrete neuronal populations throughout the adult mouse brain. Prominent areas of neuronal METRN expression include the superior colliculus (*A–C*), ocular motor nucleus (*D–F*), and raphe nucleus (*G, H*). *A* Prominent population of neurons in the superior colliculus expressing METRN. *B* Boxed area from *A* shown at greater magnification illustrates clear neuronal morphology of METRN⁺ cells. *C* A number of the METRN⁺ cells (*green*) in the superior colliculus also expressed GABA (*red*; *arrowheads*). *Boxed area* shown as single color channels to demonstrate overlap (*C'–C''*). *D* Large neurons in the ocular motor nucleus expressed METRN. *E* *Boxed area* from *D* shown at greater magnification. *F* Virtually all METRN⁺ cells (*green*) in the ocular motor nucleus expressed ChAT.

(red), boxed area shown as single color channels to demonstrate overlap ($E''-F''$). G METRN+ neurons can be found throughout the raphe nucleus (*Rph*, dorsal raphe nucleus pictured here) and also in the pontine nuclei (*Pons*). $H-H''$ The majority of METRN+ cells (green) in the raphe nucleus also express 5HT (red; e.g., arrowheads). $I-I''$ Neuronal expression of METRN (green) was also prominent in the thalamus, where it was diffusely expressed across the structure but at varying intensities among different thalamic nuclei. Expression was high for example in the latero-posterior thalamic nucleus (*LPNR*) and reticular nucleus (*Rt*). Calbindin+ (red) and parvalbumin+ (blue) neurons are shown to exemplify METRN distribution across different thalamic compartments. Scale bars represent 50 μ m (*A*, *C*, *D*, *F*, *G*, and *I*) and 500 μ m (*B*, *E*, and *H*).

Figure 5 Production and characterization of recombinant mouse METRN. **a** Reversed phase chromatographic and SDS-PAGE (insert) analysis of metal chelate affinity purified METRN. Chromatography was monitored at 214 nm. **B** MALDI-TOF mass spectrometric analysis of the main peak fractions from reversed phase chromatography revealing a mass center of 30,702 Da. **c** Western blot analysis of a serial dilution of purified METRN in DMEM+10% FCS using anti-METRN. **d** Recombinant METRN (1 nM) induces neurite outgrowth in dissociated DRG cultures to the same extent as NGF (1 nM). Cells incubated without addition of factor was included as negative control. Quantitative data (left) are the means \pm SEM from a representative experiment, and asterisk indicate a significant difference from the control ($P < 0.05$, one-way ANOVA, multiple comparisons versus control group, Holm-Sidak method). Images (right) are examples of control cells and cells stimulated with 1 nM METRN and NGF, respectively



after intrastriatal injection of 1.4 μg of recombinant METRN, showed a widespread distribution of METRN throughout the injected striatum and overlying cortex (Fig. 6b). The pattern of METRN diffusion in the striatum indicated an extracellular distribution, with no evidence of uptake by cells located in the striatum (Fig. 6c). In the adjacent septum and globus pallidus, on the other hand, there were numerous intensely METRN+ cells with a clear neuronal morphology (Fig. 6c, d). This observation indicates cellular uptake of recombinant METRN as there was no corresponding signal in uninjected control animals (data not shown). The injected HIS-tagged protein could also be detected with anti-HIS antibodies, but the signal to noise ratio was much lower compared to anti-Meteorin (data not shown).

In animals receiving intrastriatal injections of lentivirus encoding METRN, intensely METRN+ cells could be

observed around the injection site along with a more broadly distributed METRN immunoreactivity indicative of extracellular METRN protein (Fig. 6e, f). Transduced cells were predominately neurons, although a number of METRN+ glial cells were also observed around the injection site (Fig. 6g). Consistent with transduction of striatal projection neurons and subsequent anterograde transport, METRN+ fibers could clearly be traced from the injection site to the globus pallidus (Fig. 6h) and substantia nigra pars reticulata (Fig. 6i).

Discussion

Using RT-PCR and Western blotting, we show that METRN expression is largely restricted to the CNS in agreement with earlier observations (Nishino et al. 2004;

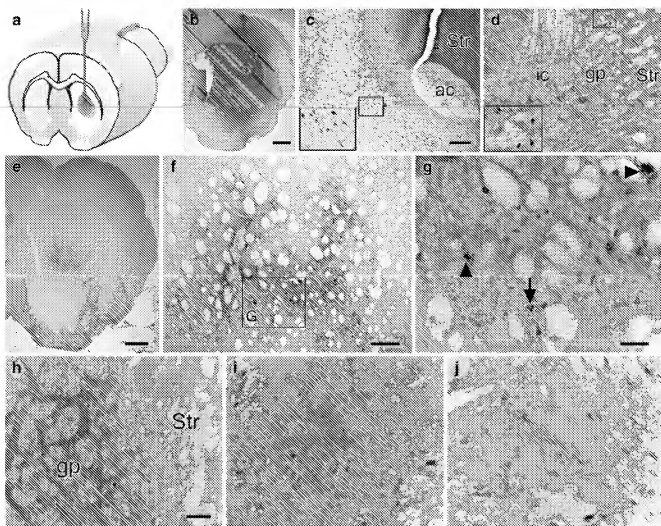


Figure 6 In vivo delivery of METRN through protein injection or lentiviral transduction. **a** Intrastriatal injection. **b–d** Immunohistochemical detection of METRN 2 h after injection of the recombinant protein. **b** A prominent level of extracellular METRN can be seen throughout the injected striatum and also in the overlying cortex. **c** Neurons in the septum ipsilateral to the injected side stained strongly for METRN (boxed area enlarged as inset illustrating neuronal profiles). Note the cellular uptake in this septal population, while the diffuse striatal signal is indicative of an extracellular METRN protein distribution. **d** Neurons in the globus pallidus also appeared intensely stained for METRN on the protein injected side of the brain (boxed area expanded as inset). **e–j** Immunohistochemical detection of METRN 2 weeks following lentiviral transduction of striatal cells. **e**

Low magnification overview showing the pattern of METRN+ signal after intrastriatal injection of LV-METRN. **f** Intensely stained METRN+ cells and a diffuse pattern of extracellular METRN could be found in and around the striatal injection site (boxed area expanded as **g**). **g** The majority of the transduced cells had a clear neuronal morphology (e.g., arrow) while a smaller number of transduced glial cells could also be observed (arrowheads). A prominent pattern of METRN+ fibers could be seen in both the globus pallidus (**h**) and the substantia nigra pars reticulata (SNr; **i**) on the injected side of the brain. **j** The background level of METRN staining is shown on the contralateral side of the SNr for comparison. **ac** anterior commissure, **gp** globus pallidus, **ic** internal capsule, **Str** striatum. Scale bars represent 500 μ m in **b** and **e**; 200 μ m in **c**, **d**, and **f**; 50 μ m in **g**, **h**, **i**, and **j**.

Park et al. 2008). It has previously been suggested that METRN expression is downregulated during brain development (Park et al. 2008), but we observed a slight increase in METRN mRNA levels throughout development and persistent expression in up to 1-year-old mice. In the adult brain, METRN mRNA is found in virtually all regions examined but at various levels. METRN protein expression in adult animals has never been investigated at the cellular

level. To be able to do this, we thoroughly tested several custom-made and commercial METRN antibodies and found that only polyclonal anti-mouse Metcorin (AF3475, R&D Systems) was useful for IHC in our hands. Using this antibody for a detailed analysis of the adult mouse brain, high levels of METRN protein in Bergmann glia were revealed, but also several discrete neuronal populations, such as the superior colliculus, the ocular motor nucleus,

the raphe and pontine nuclei, and various thalamic nuclei expressed METRN. In addition to these discrete cell populations, we also found low levels of METRN in S100 β astrocytes distributed throughout the brain. Some of these were associated with blood vessels in concordance with the METRN positive cells in the P7 cortex recently described by Park et al. (2008). However, in our study, this was clearly a subset of a broader population of METRN expressing glia distributed throughout the brain. It is not likely that the low signal from astrocytes is background as we observe a very similar stellate morphology compared to Park with a different antibody. Consistently, we also observed METRN protein throughout the brain in Western blot analysis supported by RT-PCR analysis of the same tissues. According to Nishino and co-workers, METRN mRNA is found exclusively in the Purkinje cell layer of the adult mouse brain (Nishino et al. 2004). Our detailed IHC analysis of the adult mouse brains confirms that this expression is by Bergmann glia in this layer but also reveals several additional cell populations expressing METRN. None of the neuronal populations or the ubiquitous astrocyte expression disclosed in our study is apparent in the Allen Brain Atlas (Lein et al. 2007).

To study the secretion, processing, and biochemistry of METRN, recombinant HIS-tagged protein was made and purified. We found that mature mMETRN-HIS is a 30.7-kDa monomer with the expected N-terminal and without any posttranslational modifications. Since METRN migrates according to the expected size in the tissue Western analysis, it is most likely also an unmodified monomer in vivo. As METRN has been reported to induce axonal outgrowth in E12.5 explant and E14.5 dissociated dorsal root ganglia (DRG) cultures from mouse (Nishino et al. 2004), we tested the recombinant protein in similar cultures to validate bioactivity. Indeed, METRN induces neurite outgrowth in dissociated DRG cultures from P5 rats which also indicates that METRN may play a functional role postnatally.

It is anticipated that therapeutic applications of METRN may involve the local application of protein to diseased neurons in the CNS using encapsulated cell biodelivery, gene therapy, or convection enhanced delivery as this appears necessary for other growth factors such as glial-derived neurotrophic factor (GDNF) and NGF as described in applications in Parkinson's (Lindvall and Wahlberg 2008) and Alzheimer's disease (Tuszynski 2007), respectively. To prepare for functional testing of METRN in animal models, in vivo delivery and diffusion was investigated by protein and lentiviral striatal injection. In the protein-injected animals, METRN readily diffuses and covers the entire striatum within a few hours. Compared to GDNF family members (Hamilton et al. 2001), METRN diffusion is more efficient, which may be due to the lack of

heparin-binding sites. We saw no evidence of METRN uptake by cells located in the striatum but in the adjacent septum and globus pallidus, there were numerous intensely labeled METRN-positive neurons which were not present in uninjected control animals. This could be due to internalization of METRN and one could speculate that the receptor should be found on these cells. Likewise, the lentiviral delivery showed robust intrastriatal METRN immunoreactivity and the in vivo gene therapy-characteristic "ectopic" secretion of METRN in the areas of striatal neuron projections due to intraneuronal anterograde transport of METRN and secretion by the nerve terminals. Whether a single dose or sustained delivery is preferred, both forms of delivery are possible with METRN. To do protein infusion, further studies are needed on the functional stability of recombinant METRN.

Most growth factors are members of a family, and conservation of cysteine residues is often a marked feature of such families (Sun and Davies 1995). Together with METRN, the undescribed Meteorin-like (GenID: 210029) constitutes a novel family of well-conserved secreted factors. The identity between the two family members are approximately 40% and all ten cysteine residues in the mature sequences are conserved. Analysis of EST and genome sequences from various organisms suggests orthologues for Meteorin-like in all vertebrates including zebrafish and the frog *Xenopus tropicalis*, whereas no orthologues are found in the invertebrates such as the fruit fly (*Drosophila melanogaster*) and the nematode (*Caenorhabditis elegans*). This is also the case for METRN, but here no orthologue is found in *Xenopus*. The identity between mature human and mouse METRN is 81%.

Acknowledgments This work was supported by the EU project EuroStemCell (LSHBCT-2003-503005). The Wilhelm Johansen Centre for Functional Genome Research is established by the Danish National Research Foundation. CKR is supported by Danish Stem Cell Research Doctoral School (DASDOC). The authors would like to thank Birgitte Romme Larsen, Sanne Tine Asnæs, Hanne Fosmark, Anne Klit Thomsen, Gunilla Rönholm, and Karen Friis Henriksen for excellent technical assistance and Bengt Mattsson for preparing the illustration of intrastriatal injection in Fig. 6.

References

- Bendtsen, J. D., Nielsen, H., von Heijne, G., & Brunak, S. (2004). Improved prediction of signal peptides: SignalP 3.0. *Journal of Molecular Biology*, 340, 783–795. doi:10.1016/j.jmb.2004.05.028.
- Ekesten, E. (2004). Neurotrophic factors and amyotrophic lateral sclerosis. *Neuro-Degenerative Diseases*, 1, 88–100. doi:10.1159/000080049.
- Evans, J. R., & Barker, R. A. (2008). Neurotrophic factors as a therapeutic target for Parkinson's disease. *Expert Opinion on Therapeutic Targets*, 12, 437–447. doi:10.1517/14728222.12.4.437.

- Hamilton, J. F., Morrison, P. F., Chen, M. Y., Harvey-White, J., Pernaute, R. S., Phillips, H., et al. (2001). Heparin confusion during convection-enhanced delivery (CED) increases the distribution of the glial-derived neurotrophic factor (GDNF) ligand family in rat striatum and enhances the pharmacological activity of neurturin. *Experimental Neurology*, 168, 155–161. doi:10.1006/exnr.2000.7571.
- Jensen, M. L., Timmermann, D. B., Johansen, T. H., Schousboe, A., Varming, T., & Ahring, P. K. (2002). The beta subunit determines the ion selectivity of the GABAA receptor. *The Journal of Biological Chemistry*, 277, 41438–41447. doi:10.1074/jbc.M205645200.
- Jorgensen, J. R., Juliusson, B., Henriksen, K. F., Hansen, C., Knudsen, S., Petersen, T. N., et al. (2006). Identification of novel genes regulated in the developing human ventral mesencephalon. *Experimental Neurology*, 198, 427–437. doi:10.1016/j.expneurol.2005.12.023.
- Leander, J. J., Dago, L., Tornoe, J., Rosenblad, C., & Kusk, P. (2005). A new versatile and compact lentiviral vector. *Molecular Biotechnology*, 29, 47–56. doi:10.1385/MB:29:147.
- Lein, E. S., et al. (2007). Genome-wide atlas of gene expression in the adult mouse brain. *Nature*, 445, 168–176. doi:10.1038/nature05453.
- Lindholm, P., Voutilainen, M. H., Lauren, J., Peranen, J., Leppanen, V. M., Andresson, J. O., et al. (2007). Novel neurotrophic factor CDFN protects and rescues midbrain dopamine neurons in vivo. *Nature*, 448, 73–77. doi:10.1038/nature05957.
- Lindvall, O., & Wahlberg, L. U. (2008). Encapsulated cell biodelivery of GDNF: A novel clinical strategy for neuroprotection and neuroregeneration in Parkinson's disease. *Experimental Neurology*, 209, 82–88. doi:10.1016/j.expneurol.2007.08.019.
- Nakari-Setälä, T., Aro, N., Kalkkinen, N., Alatalo, E., & Penttinen, M. (1996). Genetic and biochemical characterization of the Trichoderma reesei hydrophobin HFBI. *European Journal of Biochemistry*, 235, 248–255. doi:10.1111/j.1432-1033.1996.00248.x.
- Nishino, J., Yamashita, K., Hashiguchi, H., Fujii, H., Shimazaki, T., & Hamada, H. (2004). Meteorin: A secreted protein that regulates glial cell differentiation and promotes axonal extension. *The EMBO Journal*, 23, 1998–2008. doi:10.1038/sj.emboj.7600202.
- Park, J. A., Lee, H. S., Ko, K. J., Park, S. Y., Kim, J. H., Choe, G., et al. (2008). Meteorin regulates angiogenesis at the gliovascular interface. *Glia*, 56, 247–258. doi:10.1002/glia.20600.
- Poutanen, M., Salusjarvi, L., Ruohonen, L., Penttilä, M., & Kalkkinen, N. (2001). Use of matrix-assisted laser desorption/ionization time-of-flight mass mapping and nanospray liquid chromatography/electrospray ionization tandem mass spectrometry sequence tag analysis for high sensitivity identification of yeast proteins separated by two-dimensional gel electrophoresis. *Rapid Communications in Mass Spectrometry*, 15, 1685–1692. doi:10.1002/rcm.424.
- Schindowski, K., Belarbi, K., & Bucci, L. (2008). Neurotrophic factors in Alzheimer's disease: Role of axonal transport. *Genes Brain & Behavior*, 7(Suppl 1), 43–56.
- Shevchenko, A., Wilm, M., Vorm, O., & Mann, M. (1996). Mass spectrometric sequencing of proteins silver-stained polyacrylamide gels. *Analytical Chemistry*, 68, 850–858. doi:10.1021/ac950914h.
- Slemmon, J. R., Danho, W., Hempstead, J. L., & Morgan, J. I. (1985). Cerebellin: A quantifiable marker for Purkinje cell maturation. *Proceedings of the National Academy of Sciences of the United States of America*, 82, 7145–7148. doi:10.1073/pnas.82.20.7145.
- Sun, P. D., & Davies, D. R. (1995). The cystine-knot growth-factor superfamily. *Annual Review of Biophysics and Biomolecular Structure*, 24, 269–291. doi:10.1146/annurev.bb.24.060195.001413.
- Thompson, L., Barraud, P., Andersson, E., Kirik, D., & Björklund, A. (2005). Identification of dopaminergic neurons of nigral and ventral tegmental area subtypes in grafts of fetal ventral mesencephalon based on cell morphology, protein expression, and efferent projections. *The Journal of Neuroscience*, 25, 6467–6477. doi:10.1523/JNEUROSCI.1676-05.2005.
- Tuszynski, M. H. (2007). Nerve growth factor gene delivery: Animal models to clinical trials. *Developmental Neurobiology*, 67, 1204–1215. doi:10.1002/dneu.20510.
- Ylonen, A., Rinne, A., Hertsuain, J., Bogwald, J., Jarvinen, M., & Kalkkinen, N. (1999). Atlantic salmon (*Salmo salar* L.) skin contains a novel kininogen and another cysteine proteinase inhibitor. *European Journal of Biochemistry*, 266, 1066–1072. doi:10.1046/j.1432-1327.1999.00950.x.